CORPUS PUBLISHERS

Journal of Mineral and Material Science (JMMS)

ISSN: 2833-3616

Volume 6 Issue 6, 2025

Article Information

Received date : September 25, 2025

Published date: October 16, 2025

*Corresponding author

Freddy H Escobar, Universidad Surcolombiana, Petroleum Engineering Department, Colombia

DOI: 10.54026/JMMS/1128

Key Words

TDS-Based Methodology; Reservoirs; Petrophysical Properties; Graphical Curve

Nomenclature

Bo	Formation volume factor, rb/STB
C	Wellbore storage coefficient, bbl/psi
ct	Total compressibility, psi-1
k	Permeability, md
h	Reservoir thickness, ft
R	Radius to the discontinuity, ft
P	Pressure, psi
q	Flow rate, bpd
r	Interwell radius, ft
rw	Wellbore radius, ft
s	Time variable in Laplace space.
S	Skin
t	Time, hr
tD	Dimensionless time
tD*PD'	Dimensionless pressure derivative function, psi
(t*ΔP')	Pressure derivative function, psi

Greek Symbols

λ	Mobility ratio, dimensionless
φ	Porosity, fraction
η	Diffusivity ratio, dimensionless
μ	Viscosity, cp

Suffixes

INT	Intercept
2	Zone 2
D	Dimensionless
r	Radial
1	Zone 1

Research Article

A Practical TDS-Based Methodology for Interference Test Interpretation: A Unified Normalization Framework for Composite Reservoirs

Freddy H Escobar* and Juan Pablo Salazar

Universidad Surcolombiana, Petroleum Engineering Department, Colombia

Abstract

This work applies Tiab's Direct Synthesis (TDS) methodology to the interpretation of interference tests in composite reservoirs. By normalizing pressure and pressure-derivative curves with respect to mobility ratio (λ), diffusivity ratio (η), interwell spacing (r), and discontinuity radius (R), a unique intersection point was identified in log-log coordinates. From this point, a practical expression was formulated to estimate the discontinuity radius without resorting to conventional type-curve matching. The methodology was validated through synthetic examples, showing that the proposed approach provides reliable estimates of reservoir parameters with errors below 15%, thus offering a robust and simplified alternative for characterizing composite systems in pressure transient analysis.

Introduction

Traditionally, the interpretation of interference tests has relied on several methodologies, such as type-curve matching and the conventional straight-line method. One of the first authors to introduce the concept of interference between fields was [1], who studied how one field affects another through a shared aquifer by transcribing the pressure drop from the active field to the adjacent one through simplified material balance. The use of P_D' in the analysis of interference tests was first introduced by Tiab & Kumar [2], with the purpose of primarily estimating transmissibility without the use of type curves. Authors such as Deruyck et al. [3] presented a systematic method for interpreting interference tests in dual-porosity reservoirs; they developed and compared two models, namely pseudo-steady interporosity flow [4] and transient interporosity flow [5,6], deriving solutions in Laplace space and producing type curves for an observation well with the active well operating at either constant rate or constant pressure. Subsequently, [7] proposed an approach based on the Exponential Integral Function (Ei), which facilitated the analysis of k and c_t. One of the most innovative techniques for transient pressure analysis, including interference tests, is the *TDS* methodology ([8], introduced by [9]; it is based on a direct analytical solution that works with characteristic points of the log-log plot of pressure and its derivative function, thus improving the identification of flow regimes and the verification of results in short tests, becoming a milestone in test interpretation. Since then, its scope has expanded to fractured and horizontal wells, systems with multiple boundaries or anisotropy, and elongated or composite reservoirs [10]. Escobar et al. [10] extended the TDS methodology proposed by Tiab [9] to multiwell interference tests, proposing to read the intersection point of the log-log plot of pressure and its derivative versus time; based on that reading, he formulated expressions to estimate properties such as average horizontal permeability. More recently, Escobar et al. [11] applied the *TDS* methodology under linear and spherical flow conditions and formulated direct analytical expressions for interpretation.

Building upon this foundation, the *TDS* technique was implemented for the interpretation of interference tests in composite reservoirs. During the 1960s, several authors proposed the first analytical solutions to mathematically represent two-region concentric systems, analyzing pressure behavior in composite reservoirs for slightly compressible fluids, and establishing parameters such as discontinuity radius and inner-region property ratios. [12] later addressed the case of circular bounded reservoirs, further advancing the understanding of transient pressure behavior in infinite systems. The model developed in the present work traces back to [13], who introduced a single injector-producer scheme in thermal recovery processes, where region 1 (the inner zone) corresponds to the area invaded by steam or air (with R representing the distance from the injector well to the injection front), whereas region 2 is represented by the zone ahead of the injection front, where a slightly compressible fluid is considered. Their solution, formulated in Laplace space and inverted numerically using [14] algorithm, was subsequently extended in the same year by Satman [13] to applications beyond thermal recovery, as previously studied by Kazemi H [15], Ultimately, Satman A [16]] expanded the model to interference testing, proposing a producer or injector well at the center of two concentric regions and an observation well. Here, a mathematical expression is presented, which is highly useful for determining the radius from the producer or injector well to the discontinuity limit, expressed in the formulation as R. This expression was synthesized through the normalization of D curves which, together with other expressions proposed for the *TDS* method, were applied in synthetic cases, with the purpose of evidencing the relevance of characterizing composite reservoirs and delimiting the method's limitations.

Mathematical Model

The mathematical model adopted in this study corresponds to the one developed by Satman A [17] for composite reservoirs, and its analytical solution, Equation (1), allows for the numerical solution of the flow equations in systems with two zones of different petrophysical properties. The main assumptions are: slightly compressible single-phase flow; negligible gravitational effects; horizontal formation with constant thickness; infinite external boundary; and two concentric zones with distinct properties (inner region 1 and outer region 2). Likewise, the *D* definitions of λ, η, R_D, r_D, C_D y *S* are employed.

$$\bar{p}_{2D} = \frac{K_0(r_D\sqrt{s})}{s^{3/2}R_D\left[A\lambda K_0(R_D\sqrt{s}) - BK_1(R_D\sqrt{s})\right]} \quad (1)$$

$$A = \alpha_{11} K_1(R_D\sqrt{s\eta}) + \alpha_{12} I_1(R_D\sqrt{s\eta}) \quad (2)$$

$$B = \alpha_{11} K_0(R_D\sqrt{s\eta}) + \alpha_{12} I_0(R_D\sqrt{s\eta}) \quad (3)$$

$$\alpha_{11} = \frac{c_D}{\eta} s\left[I_0(\sqrt{s\eta}) - S\sqrt{s\eta} I_1(\sqrt{s\eta})\right] - \sqrt{s\eta} I_1(\sqrt{s\eta}) \quad (4)$$

$$\alpha_{12} = \frac{c_D}{\eta} s\left[K_0(\sqrt{s\eta}) + S\sqrt{s\eta} K_1(\sqrt{s\eta})\right] + \sqrt{s\eta} K_1(\sqrt{s\eta}) \quad (5)$$

where the terms I_0, I_1, K_0 and K_1 are modified Bessel functions and the previously introduced D variables are defined as follows:

$$P_{2D} = \frac{k_2 h \Delta P}{141.2 q \mu B} \quad (6)$$

$$t_D * P_{2D}{}' = \frac{k_2 h (t*\Delta P')_2}{141.2 q \mu B} \quad (7)$$

$$t_{2D} = \frac{0.0002637 k_2 t}{(\phi \mu c_t)_2 r_w^2} \quad (8)$$

$$r_D = \frac{r}{r_w} \quad (9)$$

$$R_D = \frac{R}{r_w} \quad (10)$$

$$C_D = \frac{C}{2\pi h (\phi c_t)_1 r_w^2} \quad (11)$$

The diffusivity and mobility ratios are defined by:

$$\eta = \frac{\left(\frac{k_1}{\phi_1 \mu_1 c_{t1}}\right)}{\left(\frac{k_2}{\phi_2 \mu_2 c_{t2}}\right)} \quad (12)$$

$$\lambda = \frac{\left(\frac{k_1}{\mu_1}\right)}{\left(\frac{k_2}{\mu_2}\right)} \quad (13)$$

According to [9] the reservoir permeability is obtained form the r flow regime by:

$$k_2 = \frac{70.6 q \mu B}{h (t*\Delta P)_{r_2}} k_2 = \frac{70.6 q \mu B}{h (t*\Delta P)_{r_2}} \quad (14)$$

TDS Methodology

TDS technique allows the interpretation of pressure well tests by using characteristic points and lines found on the pressure and pressure derivative versus time log-log plot, [9]. For this purpose, simulations were performed using different values of (λ, η, r, R), which made it possible, from the log-log plot of the D pressure and pressure derivative function, to identify a unique characteristic intersection point that served as the basis for the formulation of the equation reported in this project.

In the simulations, values of λ ranging from 0.25 to 2 were used, while keeping the remaining variables (η, R_D, r_D) constant. The resulting curves are shown in Figure 1. The adjustment consisted of scaling the abscissa axis as $t_D/\lambda^{0.035}$ and the ordinate axis as (P_D *and* t_D*P_D')$/\lambda^{0.015}$. The result of this normalization is presented in Figure 2. For diffusivity (η), values ranging from 0.25 to 2 were used, while keeping the remaining variables (λ, R_D, r_D) constant. The resulting curves are shown in Figure 3. The adjustment consisted of scaling the abscissa axis as $t_D/\eta^{0.035}$ and the ordinate axis as (P_D *y* t_D*P_D')$/\eta^{0.015}$. The result of the applied normalization is shown in Figure 4.

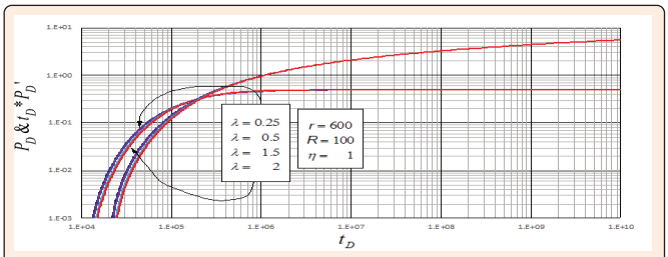

Figure 1: Effect of the mobility ratio (λ) on the behavior of dimensionless pressure and pressure derivative function for composite reservoirs.

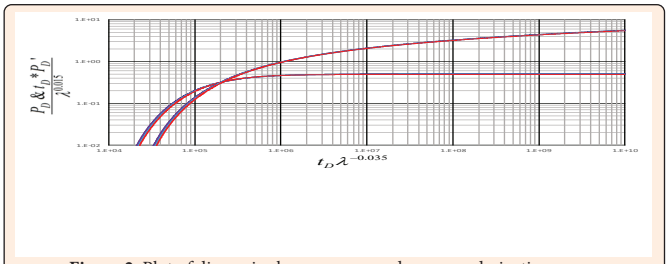

Figure 2: Plot of dimensionless pressure and pressure derivative versus dimensionless time, normalizing of the different curves for the mobility ratio λ values.

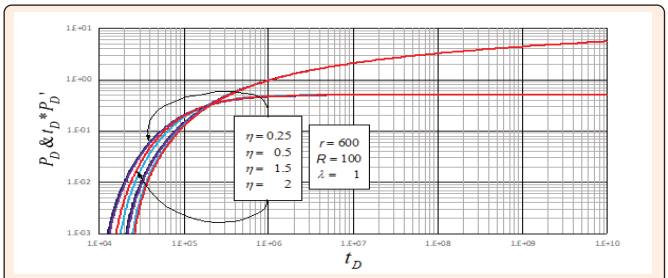

Figure 3: Effect of the diffusivity ratio (η) on the behavior of dimensionless pressure and pressure derivative function for composite reservoirs.

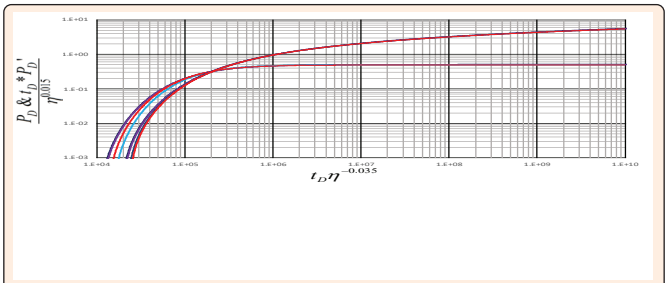

Figure 4: Plot of dimensionless pressure and pressure derivative versus dimensionless time, normalization of the different curves for the diffusivity ratio (η) values.

To observe the effect of the well spacing *(r)*, values ranging from 200 to 800 were used, while keeping the remaining variables *(λ, R_D, η)* constant. The resulting curves are shown in Figure 5. The adjustment consisted of scaling the abscissa axis as $t_D/r_D^{2.25}$ and the ordinate axis as $(P_D \text{ y } t_D{*}P_D')/ r_D^{0.09}$. The result of the applied normalization is shown in Figure 6. For the development of the equation to find the distance to the discontinuity were used, while keeping the remaining variables *(λ, η, r_D)* constant. The resulting curves are shown in Figure 7. The adjustment consisted of scaling the abscissa axis as $t_D/R^{0.2}$ and the ordinate axis as $(P_D$ and $t_D{*}P_D')/ R^{0.08}$. The result of the applied normalization is shown in Figure 8.

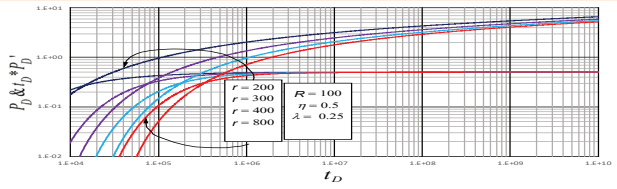

Figure 5: Effect of well spacing (r) on the behavior of dimensionless pressure and pressure derivative function for composite reservoirs.

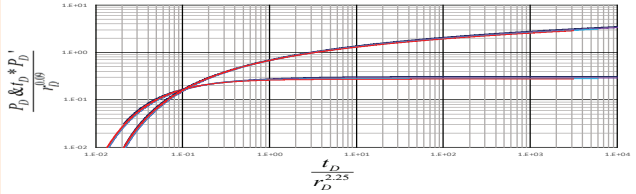

Figure 6: Plot of dimensionless pressure and pressure derivative versus dimensionless time, normalization of the different curves for the well spacing (r) values.

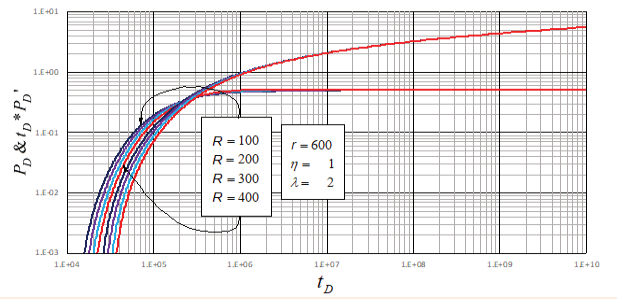

Figure 7: Effect of the discontinuity radius (R) on the behavior of dimensionless pressure and pressure derivative function for composite reservoirs.

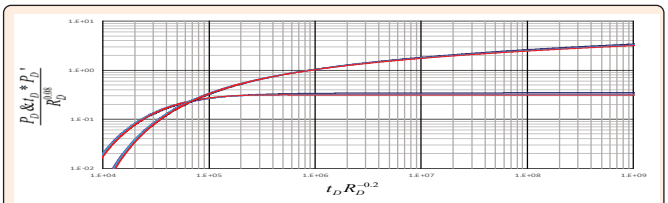

Figure 8: Plot of dimensionless pressure and pressure derivative versus dimensionless time, normalization of the different curves for the discontinuity radius (R) values.

Finally, the series of each variable studied *(λ, η, r_D, r)* were combined and plotted together, as shown in Figure 9. Based on the adjustments obtained for each variable, the normalization was defined as follows: on the abscissa axis *(λ, η, r_D, r)*, and on the ordinate axis $(P_D \text{ y } t_D{*}P_D')/ (\lambda^{0.015} \eta^{0.015} R_D^{0.09} r_D^{0.08})$. Under this normalization, the curves of P_D and $t_D{*}P_D'$ exhibit a unique intercept point, $(t_D)_{INT} = 0.045$, as shown in Figure 10.

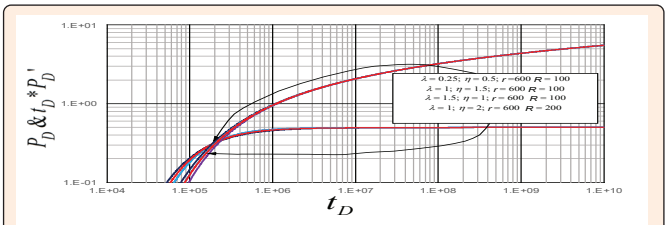

Figure 9: Plot of dimensionless pressure and pressure derivative versus dimensionless time for different data sets of *(R, r, λ, η)*.

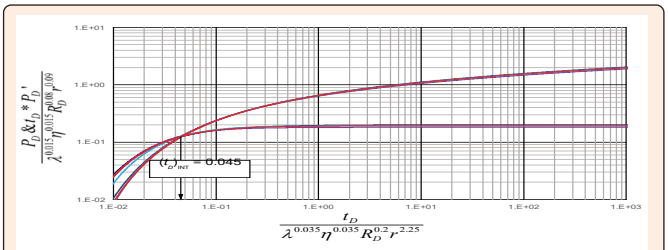

Figure 10: Plot of dimensionless pressure and pressure derivative versus dimensionless time, consolidated for different data sets of *(R, r, λ, η)*.

For the development of the equation to find the distance to the discontinuity, the normalization performed with the four variables (λ, η, r_D, r) and the identified INT point were considered; thus, $(t_D)_{INT} = 0.045$. Then, from Figure 10:

$$0.045 = \frac{(t_D)_{INT}}{\lambda^{0.035}\eta^{0.035}R_D^{0.2}r_D^{2.25}} \quad (15)$$

Substition of Equations (8), (9) and (10) and solving for R, it yields: Nótese que t_D canbe substituted using the equation 17). Where t becomes (t)INT, and rD can be substituted using the equation 20 respectively, thus obtaining:

$$R_D = 6.91016\times 10^{-12} \times \left(\frac{k_2 t_{INT} r_w^{0.25}}{(\phi\mu c_t)_2 \lambda^{0.035}\eta^{0.035}r_D^{2.25}}\right)^5 \quad (16)$$

Simulated Examples

Synthetic Example 1

There is an interference test conducted between Well 1 and Well 2, the latter being shut-in. Determine the radius at which Zone 1 ends.

q = 100 BPD	r_w = 0.5 ft	B_o = 1.25 rb/stb	$\phi_1\phi_1$= 0.35
$\mu_1\mu_1$= 1 cp	$\mu_2\mu_2$=1 cp	k_1 = 100 md	$\phi_2\phi_2$= 0.15
c_{t2}= 1x10^{-5} psi^{-1}	c_{t1} = 1x10^{-5} psi^{-1}	h = 100 ft r = 500 ft	

From the log-log plot of pressure and the pressure derivative function versus time, shown in Figure 11, the following information is obtained:

$(t^*\Delta P')_{t2}$ = 0.252 psi $\quad$ t_{INT} = 2.6384 hr

Use Equation 154 to determine permeability,

$$k_2 = \frac{(70.6)(100)(1)(1.25)}{(100)(0.252)} = 350.20\text{md}$$

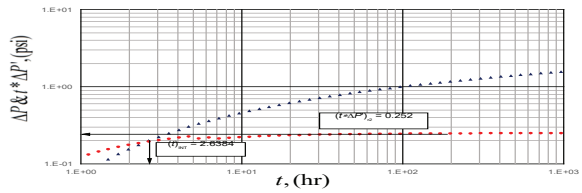

Figure 11: Pressure and pressure derivative versus time log-log plot for synthetic example 1.

Subsequently, we can determine both our mobility ratio and diffusivity ratio using Equations (12) and (13), thus obtaining:

$$\eta = \frac{\left(\frac{100}{(0.35)(1)(1\times 10^{-5})}\right)}{\left(\frac{350.20}{(0.15)(1)(1\times 10^{-5})}\right)} = 0.12238$$

Finally, Equation (16) is used in order to determine the radius R_D:

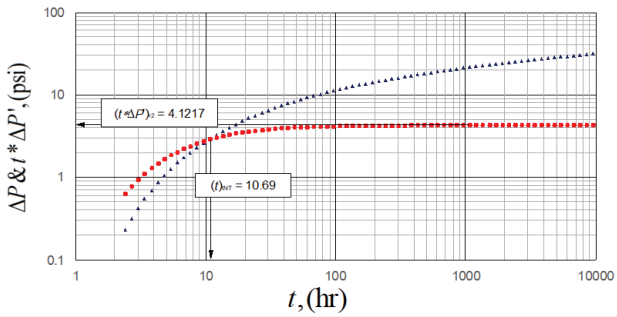

Figure 12: Pressure and pressure derivative versus time log-log plot for synthetic example 2.

$$R_D = 6.91016\times 10^{-12} \times \left(\frac{(350.20)(2.6384)(0.5)^{0.25}}{(0.15)(1)(0.00001)(0.28555)^{0.035}(0.12238)^{0.035}(500)^{2.25}}\right)^5 = 200.64376$$

Synthetic Example 2

There is an interference test conducted between Well 1 and Well 2, the latter being shut-in. Determine the radius at which Zone 1 ends.

q = 100 BPD	r_w = 0.5	B_o = 1.25 rb/stb	$\phi_1\phi_1$= 0.20
$\mu_1\mu_1$= 1.5 cp	$\mu_1\mu_1$=1.5 cp	k_1 = 200 md	$\phi_2\phi_2$= 0.15
c_{t2}= 1x10^{-5} psi^{-1}	c_{t1} = 1x10^{-5} psi^{-1}	h = 30 ft	r =450 ft

From the log-log plot of pressure and the pressure derivative function versus time, shown in Figure 12, the following information is obtained:

$(t^*\Delta P')_{t2}$ = 4.1217 psi $\quad$ t_{INT} =10.69 hr

The permeability of zone 2 is estimated using Equation (14),

$$k_2 = \frac{(70.6)(100)(1.5)(1.25)}{(30)(4.1217)} = 107.055\text{md}$$

Subsequently, the mobility ratio and diffusivity ratio can be determined using Equations (12) and (13), respectively, yielding:

$$\eta = \frac{\left(\frac{200}{(0.15)(1.5)(1\times 10^{-5})}\right)}{\left(\frac{107.055}{(0.20)(1.5)(1\times 10^{-5})}\right)} = 1.401$$

Finally, the obtained data are applied to Equation (16) to determine the radius affected by the stimulation:

$$R_D = 6.91016\times 10^{-12} \times \left(\frac{(107.055)(10.69)(0.5)^{0.25}}{(0.15)(1.5)(0.00001)(1.868)^{0.035}(1.401)^{0.035}(450)^{2.25}}\right)^5 = 118.42$$

Comments on the Results

The consistency of the proposed TDS methodology for interference testing in composite reservoirs was evaluated by verifying the collapse of the P_D and $t_D{}^*P_D{}'$ curves under the joint normalization of (λ, η, r, R), and by confirming the existence of a unique intersection point in the log-log plane. The INT obtained was $(t_D)_{INT}$ = 0.045 when the abscissa axis was scaled as $t_D/(\lambda^{0.035}\eta^{0.035}R_D{}^{0.2}r_D{}^{2.25})$, , and the ordinates as $(P_D \text{ and } t_D{}^*P_D{}')/(\lambda^{0.015}\eta^{0.015}R_D{}^{0.08}r_D{}^{0.09})$.

A practical expression was derived to estimate R without resorting to type curves. Verification with synthetic cases generated by the software showed an error of less than 20% in the calculation of R, which is considered acceptable for interference test interpretation purposes.

It was also observed that normalization loses efficiency for very high contrasts in properties such as λ >10 and η >10. In such scenarios, curve collapse weakens and the equation exhibits greater bias. For this reason, the methodology could not be applied to the case proposed in Satman's example, where λ >10 y η >10, corresponding to a gas injection scenario.

Conclusion

The application of the *TDS* methodology to interference tests in composite reservoirs enabled the formulation of a practical expression to estimate the discontinuity radius. This approach eliminates the need for type-curve matching and provides a direct means to characterize heterogeneous systems. Synthetic case studies demonstrated that the methodology is capable of reproducing reservoir behavior with acceptable accuracy, yielding errors of less than 20% in the estimation of discontinuity radius. These results confirm the robustness and reliability of the proposed normalization approach. The study highlights the usefulness of *TDS* as a simplified and consistent tool for interpreting interference tests in composite reservoirs. By improving parameter estimation while reducing dependence on graphical curve matching, the methodology strengthens the practical applicability of pressure transient analysis in complex reservoir systems.

References

1. Satman A, Mauricio E, Tang R WK, Ramey HJ (1980) An analytical study of transient flow in systems with radial discontinuities. SPE Annual Technical Conference and Exhibition SPE-9399-MS.
2. Hurst W (1960) Interference between oil fields. Transactions of the AIME 219(01): 175-192.
3. Tiab D, Kumar A (1980) Application of the p'D function to interference analysis. Journal of Petroleum Technology 32(08): 1465-1470.
4. Deruyck BG, Bourdet DP, DaPrat G, Ramey HJ (1982) Interpretation of interference tests in reservoirs with double porosity behavior-Theory and Field Examples. SPE Annual Technical Conference and Exhibition, SPE-11025-MS.
5. Warren JE, Root PJ (1963) The behavior of naturally fractured reservoirs. Society of Petroleum Engineers Journal 3(03): 245-255.
6. De Swaan OA (1976) Analytic solutions for determining naturally fractured reservoir properties by well testing. Society of Petroleum Engineers Journal 16(03): 117-122.
7. Kazemi H (1969) Pressure transient analysis of naturally fractured reservoirs with uniform fracture distribution. Society of Petroleum Engineers Journal 9(04): 451-462.
8. Al-Marhoun MA (1985) Interference testing: A new analysis approach. Middle East Oil Technical Conference and Exhibition, SPE-13732-MS.
9. Ouandlous (1999) A Interpretation of interference test by Tiab's direct synthesis technique [Thesis]. Oklahoma University, USA.
10. Tiab D (1993) Analysis of pressure and pressure derivatives without type-curve matching: I-Skin and Wellbore Storage. SPE Production Operations Symposium SPE-25426-MS.
11. Escobar FH, Jongkittnarukorn K, Hernandez CM (2019) The power of TDS technique for well test interpretation: A short review. Journal of Petroleum Exploration and Production Technology 9(1): 731-752.
12. Escobar FH, Rojas E, Alarcón NT (2018) Analysis of pressure and pressure derivative interference tests under linear and spherical flow conditions. DYNA 85(204): 44-52.
13. Carter RD (1966) Pressure behavior of a limited circular composite reservoir. Society of Petroleum Engineers Journal 6(04): 328-334.
14. Satman A, Eggenschwiler M, Ramey HJ (1980) Interpretation of injection well pressure transient data in thermal oil recovery. SPE California Regional Meeting SPE-8908-MS.
15. Stehfest H (1970) Algorithm 368: Numerical inversion of laplace transforms [D5] Communications of the ACM 13(1): 47-49.
16. Kazemi H (1966) Locating a burning front by pressure transient measurements. Journal of Petroleum Technology 18(02): 227-232.
17. Satman A (1985a) An analytical study of interference in composite reservoirs. Society of Petroleum Engineers Journal 25(02): 281-290.
18. Satman A (1985b) An analytical study of interference in composite reservoirs. Society of Petroleum Engineers Journal 25(02): 281-290.